In Situ Detection of Salmonid Alphavirus 3 (SAV3) in Tissues of Atlantic Salmon in a Cohabitation Challenge Model with a Special Focus on the Immune Response to the Virus in the Pseudobranch

Haitham Tartor *, Lisa-Victoria Bernhardt , Saima Nasrin Mohammad , Raoul Kuiper , Simon C Weli

Posted Date: 18 October 2023

doi: 10.20944/preprints202310.1132.v1

Keywords: Atlantic salmon; Salmonid alphavirus 3 (SAV3); Pseudobranch; Immune response; Pancreas disease (PD); In situ hybridization; RNAscope®

Article

In Situ Detection of Salmonid Alphavirus 3 (SAV3) in Tissues of Atlantic Salmon in a Cohabitation Challenge Model with a Special Focus on the Immune Response to the Virus in the Pseudobranch

Haitham Tartor [1,*], Lisa-Victoria Bernhardt [2], Saima Nasrin Mohammad [1], Raoul Kuiper [3], Simon C Weli [3]

[1] Department of Fish Health, Norwegian Veterinary Institute, Ås, Norway; Haitham.tartor@vetinst.no (H.T.); saima-nasrin.mohammad@vetinst.no (S.N.M.)
[2] DNV Headquarters, Høvik, Norway; Lisa.Victoria.Bernhardt@dnv.com (L.V.B.)
[3] Department of Fish Biosecurity, Norwegian Veterinary Institute, Ås, Norway Raoul.Valentin.Kuiper@vetinst.no (R.K.); simon.weli@vetinst.no (S.C.W.)
* Correspondence: Haitham.tartor@vetinst.no; Tel.: (+4740018042)

Abstract: Salmonid alphavirus strain 3 is responsible for outbreaks of pancreas disease in salmon and rainbow trout in Norway. Although the extensive amount of research on SAV3 focused mainly on the heart and pancreas (of clinical importance), tropism and pathogenesis studies of the virus in other salmon tissues are limited. Here, we used a combination of RT-qPCR (Q_nsp1 gene) and *in situ* hybridization (RNAscope®) to demonstrate the tropism of SAV3 *in situ* in tissues of Atlantic salmon, employing a challenge model (by cohabitation). In addition, as previous results suggested that pseudobranch may harbor the virus, the change in the expression of different immune genes upon SAV3 infection (RT-qPCR) was focused on the pseudobranch in the current study. *In situ* hybridization detected SAV3 in the heart, pseudobranch, gills, pyloric caeca, and pancreas after virus infection, with the heart ventricle showing the most extensive infection. Furthermore, the detection of the virus at different adipose tissues associated with the internal organs of the salmon, suggests a specific affinity of SAV3 to adipocyte's components. The innate immune response to SAV3 in the pseudobranch after infection dominated over the adaptive responses, yet it did not mitigate the infection in that tissue. The early detection of SAV3 in the pseudobranch after infection, along with the persistent low infection over the experimental course, suggests a pivotal role of the pseudobranch in SAV3 pathogenesis in Atlantic salmon.

Keywords: Atlantic salmon; salmonid alphavirus 3 (SAV3); pseudobranch; immune response; pancreas disease (PD); in situ hybridization; RNAscope®

1. Introduction

Alphaviruses (family Togaviridae) is a diverse group of small, spherical, enveloped viruses with single-stranded, positive-sense RNA genomes [1]. Alphaviruses that infect salmonids (SAV) have three known subtypes (SAV1, SAV2, and SAV3) which cause different diseases in salmonids and have been seen as an increasing problem in the European salmonid-farming industry [2]. SAV1 is the causative agent of pancreas disease (PD) in Atlantic salmon (*Salmo salar* L.) in the British Isles [3], SAV2 causes sleeping disease (SD) in rainbow trout (*Oncorhynchus mykiss*, Walbaum) in France [4], and England [5]. SAV3 on the other hand is responsible for outbreaks of PD in Atlantic salmon and rainbow trout in Norway [6].

Salmonid alphavirus 3 tropism in Atlantic salmon has been previously studied in an experimental infection model with an atypical infection route (intraperitoneal injection [i.p.]) using RT-qPCR [2]. However, the precise in situ localization of SAV3 in infected salmon tissues has not yet been studied. Histopathological studies of PD in Atlantic salmon showed lesions predominantly in the pancreas, heart, and skeletal muscle [7]. In spite of the reported persistence of SAV3 in gills and pseudobranch [2], histopathological changes were not reported. Also the immunological studies

 doi:10.20944/preprints202310.1132.v1

addressing SAV3 infection in salmon focused on the heart, peritoneal cavity, and immune tissues (anterior kidney and spleen) [8–10]. These observations call for a more detailed investigation of the role of gills and pseudobranch in virus persistence and to evaluate whether both gills and pseudobranch, can be useful sensors for SAV infection, regardless of the PD status [11].

The pseudobranch is a reduced mandibular gill arch, situated anterodorsally in the opercular cavity of a number of teleosts [12]. The pseudobranch structure can be either a free, gill-like organ fully exposed to the water as in flounder, black goby, and Gobius niger, or a glandular organ deeply buried in the operculum tissue with fused lamellae, and no contact to the external medium as in Cyprinidae, Atlantic cod, and mature salmonids [13]. The arterial blood supply in the pseudobranch originates from the first efferent gill artery and it splits up within the pseudobranch into a capillary system, where its efferent vessel– also known as "the ophthalmic artery" – nourishes the choroid gland of the eye [14,15]. Because of this capillary network, pseudobranch plays roles in respiration, and osmoregulation, as well as in the regulation of ocular circulation, either by controlling blood pressure in the eye or by regulating the eye fluids biochemically via the choroid gland [12].

The pseudobranch was previously suggested to be involved in the pathogenesis of different diseases, including, for example, parvicapsulosis (caused by *Parvicapsula pseudobranchicola*) [16] and Varracalbmi (caused by *Pasteurella spp.*) [17] in Atlantic salmon, and Microsporidiosis (caused by *Loma salmonae*) in chinook salmon [18]. In advanced cases of infection with *Parvicapsula pseudobranchicola*, for example, a whitish "cheesy" material was found to obstruct the blood supply to the choroid bodies and impact the blood circulation of the eye and could thus be responsible for vision impairment in infected salmon [16]. Also in chinook salmon infected with Loma salmonae, circulation dysfunction due to occlusion of the pseudobranchial artery by the parasitic cysts was thought to be the reason for infarction and focal necrosis of cartilage in the lower jaw of infected fish [18]. The observations that SAV could be detected in the pseudobranch tissues of both salmonids [2] and non-salmonids (flatfish) [19] upon the experimental virus challenge, suggest a crucial role of that tissue in the virus pathogenesis.

In the current work, we demonstrated the in situ localization of SAV3 in the tissues of salmon experimentally exposed to the virus using an RNAscope protocol. We also compared the SAV load between the pseudobranch and the heart throughout the infection course using RT-qPCR. To investigate the role of salmon pseudobranch in the host response against SAV3 during the acute phase of infection, we compared the expression of fourteen genes involved in innate and adaptive immune activities and two mucin genes between SAV-infected and non-infected fish. Our results showed a virus tropism in the heart, pseudobranch, gills, pyloric caeca, and pancreas during the acute phase of the infection. In addition, the virus was also found in the adipose tissue associated with the internal organs of the salmon, suggesting a specific affinity of the virus to adipocytes. The inconsistent immune response of the pseudobranch against SAV3 could be responsible for the persistent low infection in that tissue and can suggest a role of the pseudobranch in SAV3 pathogenesis in Atlantic salmon.

2. Material and Methods

2.1. Fish

The current study was approved by the Norwegian Food safety Authority and some of the samples collected in it was part of the previously published work [20]. The post-smolt stage (average weight of 110.9 g) of Atlantic salmon (Stofnfiskur Iceland; SF Optimal) was used in the current study. The fish were reared at the fish facility at Industrial and Aquatic Laboratory (ILAB, Bergen High Technology Centre, Bergen, Norway) until the challenge. The fish were unvaccinated and pre-screened at 5 g and 15 g of size for SAVs, infectious salmon anemia virus, infectious pancreatic necrosis virus, piscine myocarditis virus, piscine orthoreovirus, and salmon gill poxvirus and showed negative results for all. The parent fish were also pre-screened for all these viruses, except for SGPV, and also showed negative results.

2.2. SAV3 Inoculum

The SAV3 inoculum used in the current study was prepared similarly to what was previously mentioned by Andersen *et al*. [21]. Briefly, heart and head kidney homogenates collected from SAV3-infected Atlantic salmon (obtained from the Hordaland region of Norway in 2004) were pooled and

 doi:10.20944/preprints202310.1132.v1

used for virus propagation. The virus was propagated in the CHSE-214 cell line (ATCC® CRL-1681™), and the cells were grown on Leibowitz's L-15 Medium (Lonza, USA), supplemented with 10% fetal bovine serum (FBS) and gentamicin at 20°C for 6 passages. Serial ten-fold dilutions of the propagated SAV3 (stock sample) were inoculated onto 24 h old CHSE-24 monolayers in 96-well plates, allowing quantification. The viral endpoint titer, measured as 50% tissue culture infective dose ($TCID_{50}$) as described by [22] was determined to be 1 x 10^6 / mL.

2.3. Experimental Challenge

To prepare SAV3 shedder fish, a total number of 45 fish were immersed in a bath with the anesthetic Finquel® vet. (100 mg/L). The fish were randomly divided into three groups (I – III; 15 fish/each). Fish were immobilized and injected intraperitoneal with SAV3 inoculum using 0.2 mL of a low-dose suspension (2 x 10^2 $TCID_{50}$/fish; group I), a high-dose suspension (2 x 10^4 $TCID_{50}$/fish; group II), or virus-free Leibovitz-L15 cell culture medium containing 2% FBS (mock inoculum; group III). The fish with low-dose, high-dose, or SAV-free were transferred into three different 500 L seawater tanks, henceforth referred to as LD, HD, and Ctr., respectively, containing 55 cohabitant fish/each, which had been transferred to the tanks two days before the challenge started. To distinguish between shedder and cohabitant fish, all shedder fish were marked by adipose fin clipping. The shedder fish remained in the tanks throughout the entire challenge period (29 days).

2.4. Experimental Tanks Management

The experimental tanks were provided with seawater originating from 105 m depth and was filtered through 20 µm drum filters and treated with UV light (135 W/ m^2). The water flow in all tanks was the same throughout the experiment, with an average flow rate of 950 L/h/tank. The water in the tank was monitored daily for temperature, salinity, and dissolved oxygen levels throughout the challenge time. During the challenge period, the LD, HD, and Ctr. tanks had dissolved oxygen saturation levels of 79 – 97%, 80 – 97%, and 79 – 86%, respectively, water temperature range of 11.7 – 12.3°C, 11.7 – 12.3°C, and 11.5 – 12.4°C, respectively, and salinity range of 34.1 – 34.5‰, 34.1 – 34.5‰ and 34.2 – 34.5‰, respectively. All tanks had a daily photoperiod of 12:12 h light and dark, provided by an automatic artificial lighting system. During the 12 hours of light, an automatic feeder dispenser fed the fish with 3 mm Nutra Olympic pellets (Skretting, Norway). The amount of food given to the fish in LD, HD, and Ctr., was between 56 –140 g, 56 –140 g, and 80 –150 g, respectively; adjusted marginally as the fish were growing, dying, or being sampled. Clinical signs, as well as mortalities, were monitored daily in the three tanks, and dead fish were removed daily and did not undergo any further analysis.

2.5. Sampling

Based on our previous experience with the SAV3 experimental challenge, fish samples were collected at 0, 7, 12, 16, 19, 20, and 29 days post-challenge (dpc). At sampling time, six cohabitant fish were randomly collected from each of the LD, HD, and Ctr. tanks at each time point. Fish were first euthanized by immersing them in a bath with an overdose of Finquel® vet. 1000 mg/g (150 mg/L), the gross pathology was evaluated. Heart (including the valves and bulbous arteriosus), and pseudobranch samples were collected for RT-qPCR in RNAlater™ Soln. (Thermo Fisher Scientific Baltics, UAB, Vilnius), and samples from the heart, pseudobranch, gills, liver, spleen, posterior kidney, pyloric caeca and pancreas were collected for *in situ* hybridization in 10% neutral buffered formalin.

2.6. RNA Isolation and cDNA Synthesis

Tissue samples in RNAlater™ (Thermo Fisher Scientific Baltics) were kept at −80°C prior to RNA extraction, which was performed by adding approximately 20 mg tissue with 180 µl ATL Lysis Buffer (Qiagen®) and 20 µl Proteinase K and incubation overnight at 56°C. Extraction was performed by using QIAcube® (Qiagen®) with the reagents from the DNeasy Blood & Tissue Kit (Qiagen®), giving an RNA elution volume of 200 µl. Isolated RNA was stored at −80°C until RT-qPCR was performed.

Preprints (www.preprints.org) | NOT PEER-REVIEWED | Posted: 18 October 2023 doi:10.20944/preprints202310.1132.v1

2.7. RT-qPCR

2.7.1. SAV Q_nsp1 Assay

The SAV3 strain was detected using the Q_nsP1 assay [23]. This broad spectrum assay detects all known SAV subtypes using primers and probe (Table 1) with final concentrations of 500 and 300 nM, respectively, and amplifies a conserved region in the 5' end of the *nsP1* gene, giving amplicons of 107 bp. Extracted RNA was automatically pipetted by Eppendorf epMotion® 5075 (Eppendorf) in duplicates, analyzed by RT-qPCR on an AriaMx machine (Agilent Technologies), and evaluated with the Agilent AriaMx Real-Time PCR software (version 1.7). Each plate included a negative control sample and an inter-plate calibrator of pure SAV3 RNA, which were both run in duplicates. The cut-off quantification cycle (Cq) value was set to 40; samples with values below this Cq in duplicates were considered positive. Samples with only one positive parallel were rerun and considered positive only with positive duplicates. The template volume was 2.0 µl RNA in a total reaction volume of 20 µl, and the RT-qPCR kit used was TaqMan® Fast Virus 1-Step Master Mix (Applied Biosystems®). The thermal program comprised reverse transcription for 5 min at 50°C and enzyme activation for 2 min at 95°C, followed by 45 cycles of 15 s at 94°C and 40 s at 60°C.

2.7.2. Salmon Genes Expression

Pseudobranch samples (n = 6) were collected from fish in the LD, HD, and Ctr. tanks at 7, 12, 16, 19, 20, and 29 dpc and analyzed for the expression of different immune genes (Table 1) using RT-qPCR. Pseudobranch stock cDNA (500 ng/µl) was diluted 1:10 to analyze the expression of *IFN-α, IFN-γ, Viperin, Mx, MHC-I, CD8a, gzma, NK-lysin, MHC-II, CD4, sIgM, mIgM,* and *EF-1 α*, whereas 1:3 dilution was used to analyze *sIgT-B, mIgT-B, Muc-2 and Muc-5*. The expression was also compared between gills and pseudobranch collected from the control fish (0 dpc) in the same cDNAa mounts. The RT-qPCR experiments were performed using the ABI 7900HT fast instrument (ThermoFisherScientific) and Brilliant III Ultra-Fast SYBR® Green QPCR Master Mix (Agilent Technologies; Cat. no. 600882). Each sample was analyzed in duplicates, using a total reaction mix volume of 20 µL per well (2 µL cDNA, 0.8 µL [400 nM] of each forward and reverse primers,10 µL of the master mix, 0.3 µL [300 nM] of ROX reference dye and 6.1 µL of nuclease free-water). The elongation factor 1α (*EF1α*) gene was used as a reference gene and non-template wells were run on each plate as a negative control. The following thermocycler conditions were used: initial denaturation (3 min at 95°C) followed by 40 cycles of denaturation (5 s at 95°C), and annealing (15 s at 60°C). The extension was performed for 5 s at 55°C. Finally, a melting curve was made by measuring the fluorescence during a temperature range of (60 – 95°C) to confirm the specificity of the end-product amplicon in the reaction. Fluorescence was measured, expressed as relative fluorescence units (RFU) and quantification cycles (Cq) for every reaction that was measured. All gene expression values (Cq values) were normalized to *Ef1α* values [24] and the relative expression of target genes was calculated using the $\Delta\Delta C_t$ method [25].

Table 1. Sequences of oligonucleotide primers used in real-time PCR.

Gene name	Primers sequences (5′- 3′)	Reference
Interferon alpha (IFN-α)	F: TGCAGTATGCAGAGCGTGTG R:TCTCCTCCCATCTGGTCCAG	[26]
Interferon gamma (IFN-γ)	F: AAGGGCTGTGATGTGTTTCTG R: TGTACTGAGCGGCATTACTCC	[27]
Virus inhibitory protein, endoplasmic reticulum-associated, interferon-inducible (viperin)	F: AGCAATGGCAGCATGATCAG R: TGGTTGGTGTCCTCGTCAAAG	[28]
Myxovirus resistance (Mx)	F:TGCAACCACAGAGGCTTTGAA A:GGCTTGGTCAGGATGCCTAAT	[29]
Major histocompatibility complex class I (MHC-I)	F:GAAGAGCACTCTGATGAGGACAG R:CACCATGACTCCACTGGGGTAG	[28]
Cluster of differentiation 8 alpha (CD8a)	F:CGTCTACAGCTGTGCATCAATCAA R:GGCTGTGGTCATTGGTGTAGTC	[28]
Granzyme A (gzma)	GGTGTTTCTAGGGGTCCACTC TGCCACAGGGACAGGTAACG	[30]
Natural killer lysin (NK-lysin)	F:TGTTCTTATGCACCACGCAA R:CGGGTATGACGCAAAACGACTA	[31]

Preprints (www.preprints.org) | NOT PEER-REVIEWED | Posted: 18 October 2023 doi:10.20944/preprints202310.1132.v1

Major histocompatibility complex class II (MHC-II)	F:CCACCTGGAGTACACACCCAG R:TTCCTCTCAGCCTCAGGCAG	[32]
Cluster of differentiation 4 (CD4)	F:GAGTACACCTGCGCTGTGGAAT R:GGTTGACCTCCTGACCTACAAAGG	[33]
Secretory immunoglobulin M (sIgM)	F:CTACAAGAGGGAGACCGGAG R:AGGGTCACCGTATTATCACTAGTT	[28]
Membrane immunoglobulin M (mIgM)	F:CCTACAAGAGGGAGACCGA R:GATGAAGGTGAAGGCTGTTTT	[34]
Secretory immunoglobulin T (sIgT-B)	F:GAATGTTTGGGACACGGAAG R:TCACATATCTTGACATGAGTTACC	[35]
Membrane immunoglobulin T (mIgT-B)	F:GAATGTTTGGGACACGGAAG R:GCTCAGTCAGTGGGATGTTCT	[36]
Mucin 2 (Muc-2)	F: CGACTGCCACAAAGCCATTAGG R: GCGTGTTGCTGCGTGTCTT	[37]
Mucin 5 (Muc-5)	F: CCGTGCTGGGAGACATTATGAAGT R: TGCTGGAGAGGGAAAGGGTAAC	[37]
Elongation factor-1alpha (EF1α)	F:TGCCCCTCCAGGATGTCTAC R:CACGGCCCACAGGTACTG	[38]
SAV3-nsp1	F: CCGGCCCTGAACCAGTT R: GTAGCCAAGTGGGAGAAAGCT Probe: FAM-5 - CTGGCCACCACTTCGA-3 -MGB	[23]

2.8. In Situ Hybridization (ISH)

We demonstrated the SAV3 localization *in situ* in tissues of infected fish to study the tissue tropism of the virus. Formalin-fixed paraffin-embedded (FFPE) sections from the heart, pseudobranch, gills, liver, spleen, posterior kidney, pyloric caeca end pancreas collected from fish in the HD and Ctrl groups at 7, 12 16, 20, and 29 dpc, were prepared. A protocol based on RNAscope technology was applied using RNAscope® 2.0 HD Red Chromogenic Reagent Kit (Advanced Cell Diagnostics Inc.). In this protocol, paired double-Z oligonucleotide probes targeting a SAV3 nucleotide stretch (region 46 to 944 bp) of the genomic RNA of Norwegian SAV isolate Hav1 (Accession number: GenBank AY604235.1), were used. A negative control probe targeting the Bacillus subtilis SMY strain gene DapB (accession number EF191515, region 414 to 862 bp; Cat. No. 310043, Advanced Cell Diagnostics) was used to subtract the background signals, and a positive control probe derived from the peptidylprolyl isomerase B (PPIB) gene of Atlantic salmon (accession number NM_001140870.2, targeting region 20 to 934 bp; Cat. No. 494421, Advanced Cell Diagnostics) was applied to confirm both the mRNA integrity in the samples and the functionality of the ISH experiment. RNAscope was performed following the manufacturer's instructions. Briefly, FFPE sections were deparaffinized in xylene and rehydrated through a series of alcohol washes. The rehydrated sections were then treated with hydrogen peroxide at room temperature for 10 min to block endogenous peroxidases. Then, the sections were boiled in a target retrieval buffer for 15 min and incubated with protease at 40 °C for 15 min. The boiled sections were hybridized with the probes specified earlier at 40 °C for 2 h and then run through a sequence of signal amplification (40 °C for 15 or 30 min) and washing steps. Finally, the hybridization signal was visualized using Fast Red stain, and all slides were counterstained using Mayer's hematoxylin (Chemi Teknikk, 5B-535) diluted in distilled water 1:1 (vol/vol) for 2 min.

2.9. Statistics

Because data were not normally distributed and different groups had unequal variances, nonparametric statistical analyses were performed using JMP software (JMP®, Version 11, SAS Institute Inc., Cary, NC, 1989 – 2007) with α value set to 0.05. While the Mann-Whitney U test was conducted to detect statistically significant differences between the *Muc-2* and *Muc-5* Cq values between the pseudobranch and the gills, the significance of the difference in the immune gene expression between the virus-challenged and control groups was determined for each gene at each time point using Kruskal-Wallis test followed by Dunn's multiple comparison test. GraphPad Prism version 6.0 (San Diego, CA, US) was used to make graphs.

Preprints (www.preprints.org) | NOT PEER-REVIEWED | Posted: 18 October 2023 doi:10.20944/preprints202310.1132.v1

3. Results

3.1. In Situ Hybridization

We studied the tropism of SAV3 *in situ* in tissues collected from cohabitant fish exposed to the high dose of the virus at different time points after the challenge, using RNAscope protocol. Our results showed no SAV3-specific signal detected in tissues analyzed before 16 dpc. Heart, pseudobranch, and pancreas showed SAV3-specific hybridization at 16, 20, and 29 dpc (Figures 1 and 2). Tissues from the gills, pyloric caeca, and its surrounding adipose tissue had the virus particles at 16 and 20 dpc (Figures 3 and 4). The virus was detected on a single occasion in the posterioir kidney after 20 days of cohabitation (Figure 5). Neither the liver nor the spleen or its surrounding adipose tissue showed any SAV3-specific hybridization at any of the time points (Figure 6).

The heart tissue had the highest SAV3-signal intensity among the other tissues examined and the hybridization signal seems to dominate the ventricle compartment (mostly in the muscle cells of both the compact and spongy myocardium layers of the heart [Figure 1F]) as compared to the atrium (Figure 1G). However, neither the bulbus arteriosus nor the epicardium showed an SAV3-specific signal (Figure 1H,I).

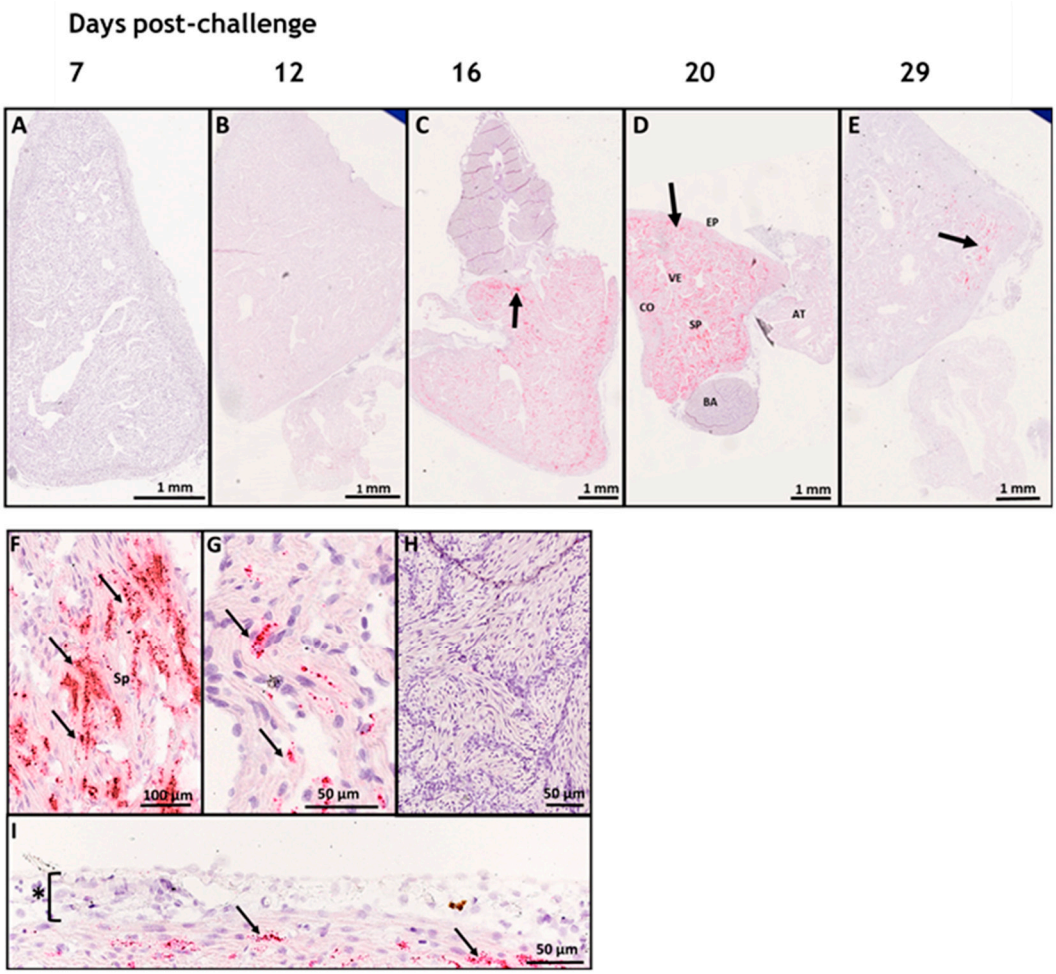

Figure 1. In situ hybridization (RNAscope) of SAV3 in the heart of Atlantic salmon challenged with the virus by the cohabitation method. Heart tissues collected from fish in the high-dose group at different time points after challenge showed SAV-specific hybridization signals (red staining and arrows). The different heart compartments (epicardium [EP], ventricle [VE], Atrium [AT], compact [CO] and spongy [SP] mycoardial layers, and bulbus arteriosus [BA]) in ◌D′ are shown on a higher magnification in ◌F – I)′. SAV-specific signal (arrows) was detected in the spongy myocardium of ventricle (F) and atrium (G) and compact myocardium of ventricle (I). No SAV-specific signal has been detected in bulbus arterious (H) or in the epicardium (* in ◌I′).

In the pseudobranch and around the virus peak (20 dpc), the signal predominates intravascularly, and seemingly in places where no circulating cells are occupying the available space

Preprints (www.preprints.org) | NOT PEER-REVIEWED | Posted: 18 October 2023 doi:10.20944/preprints202310.1132.v1

(Figure 2D,F). Furthermore, while in many places the signal appears to stick to the luminal membranes of endothelial/pillar cells, other populations of larger and irregular cells at the base of the lamellae seem to show an intracytoplasmic signal (Figure 2F).

Interestingly, SAV3-specific hybridization could also be detected in the cytoplasm of adipocytes in the adipose tissue surrounding the pseudobranch (Figure 2G). Pseudobranch sections prepared serially to those studied by RNAscope, stained with H&E, and examined for any histopathological changes that might have been caused due to SAV exposure, showed no significant histopathological alterations in areas adjacent to those where the SAV3-specific hybridization signals were detected on the RNAscope sections (Data not shown).

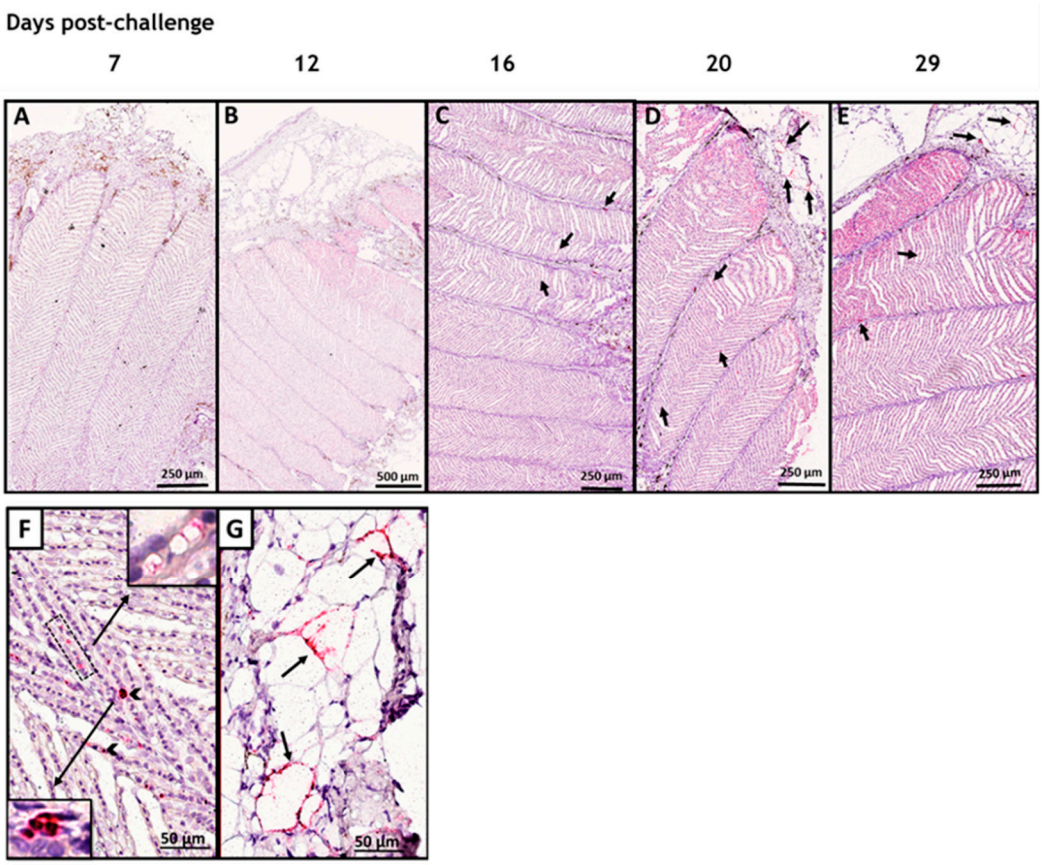

Figure 2. In situ hybridization (RNAscope) of SAV3 in pseudobranch of Atlantic salmon challenged with the virus by the cohabitation method. Pseudobranch tissues collected from fish in the high-dose group at different time points after challenge, showed SAV-specific hybridization signal (red staining and arrows) in C, D and E. The SAV-specific staining detected in ‘D’ is shown on a higher magnification in ‘F’ and ‘G’. SAV hybridization was associated with the luminal membranes of endothelial/pillar cells (dotted frame box in ‘F’), with the cytoplasm of irregular cells at the base of the lamellae (arrow head in ‘F’), and with adipocyte cytoplasm in adipose tissue around the pseudobranch (arrows in ‘G’).

As for the hybridization results of SAV3-specific probes in the gills, the signal was consistently detected in the cytoplasm of adipocytes in the gills-associated adipose tissue (Figure 3C,D,F). In addition, few of the cells running through the vascular space of the secondary lamella and in the blood vessels associated with the gills also showed a positive signal for SAV3 (Figure 3G,H). The SAV3-specific signal identified in the gill lamella was, however, less prominent as compared to that of the pseudobranch.

Preprints (www.preprints.org) | NOT PEER-REVIEWED | Posted: 18 October 2023 doi:10.20944/preprints202310.1132.v1

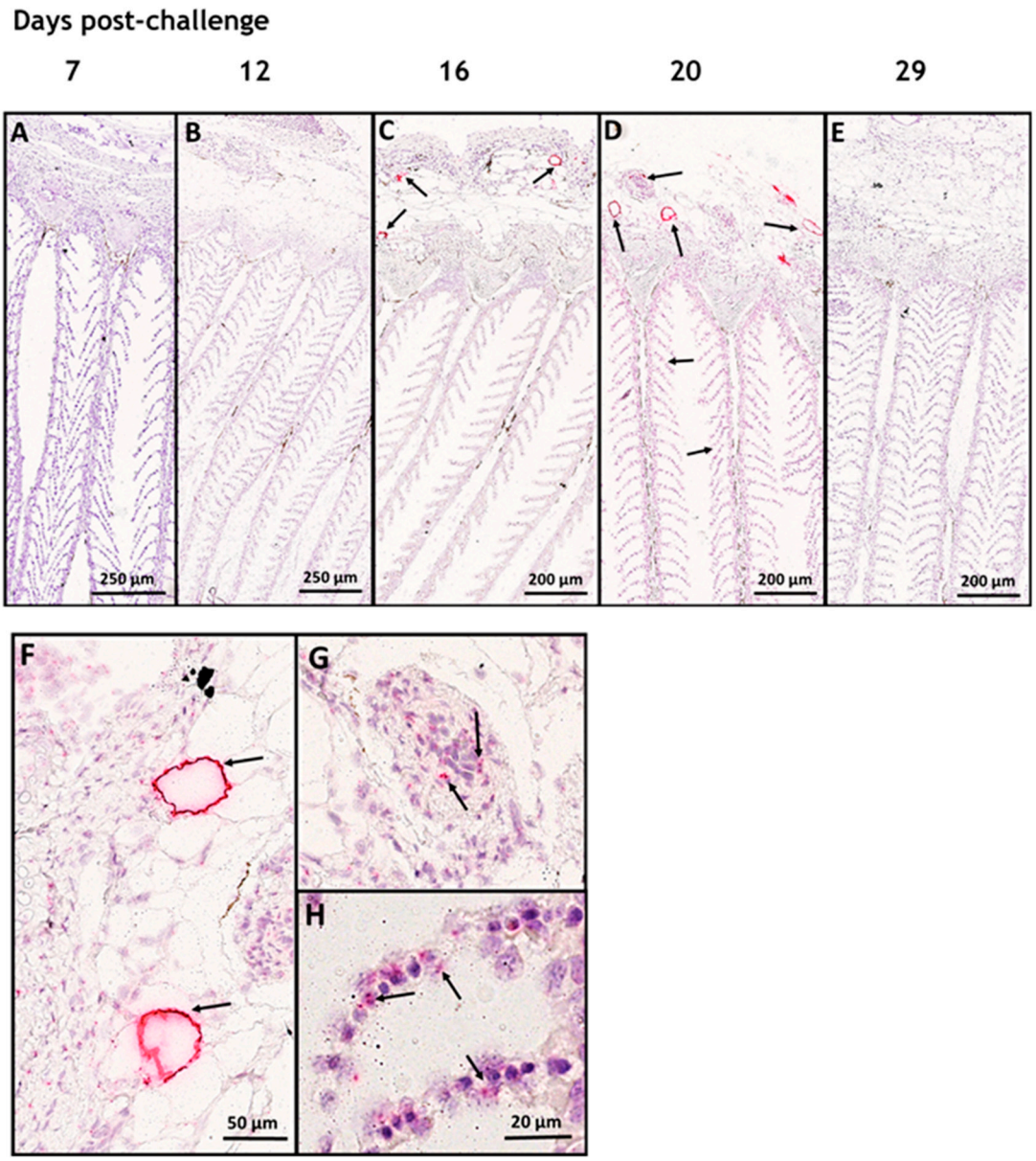

Figure 3. In situ hybridization (RNAscope) of SAV3 in gills of Atlantic salmon challenged with the virus by the cohabitation method. Gill tissues collected from fish in the high-dose group at different time points after challenge, showed SAV-specific hybridization signal (red staining and arrows) in C and D. SAV-specific staining detected in ◌D′ is shown on a higher magnification in (F – H) to show the hybridization associated with the cytoplasm of adipocytes in gills-associate adipose tissue (arrows in ◌F′), in few cells in the gill associated blood vessels (arrows in ◌G′) and in some cells running through the vascular space of the secondary lamella (arrows in ◌H′ also dotted box in ◌D′).

The SAV3-specific probes were also hybridized in the pyloric caeca and the pancreas, showing varied degrees of positivity between the virus peak time and the end of the experiment (Figure 4A–O). In the pyloric caeca, the SAV was detected in association with the columnar epithelial cells and in the mucus layer on its apical surface as well as in some cells harbored in the lamina propria of the intestinal mucosa (Figures 4C and 4D). Rare positive cells could also be detected in association with the pancreatic tissue (Figure 4H–J). As in the other tissue, the SAV3-specific signal was also detected in the cytoplasm of adipocytes surrounding the pancreas (Figure 4M,N).

Preprints (www.preprints.org) | NOT PEER-REVIEWED | Posted: 18 October 2023 doi:10.20944/preprints202310.1132.v1

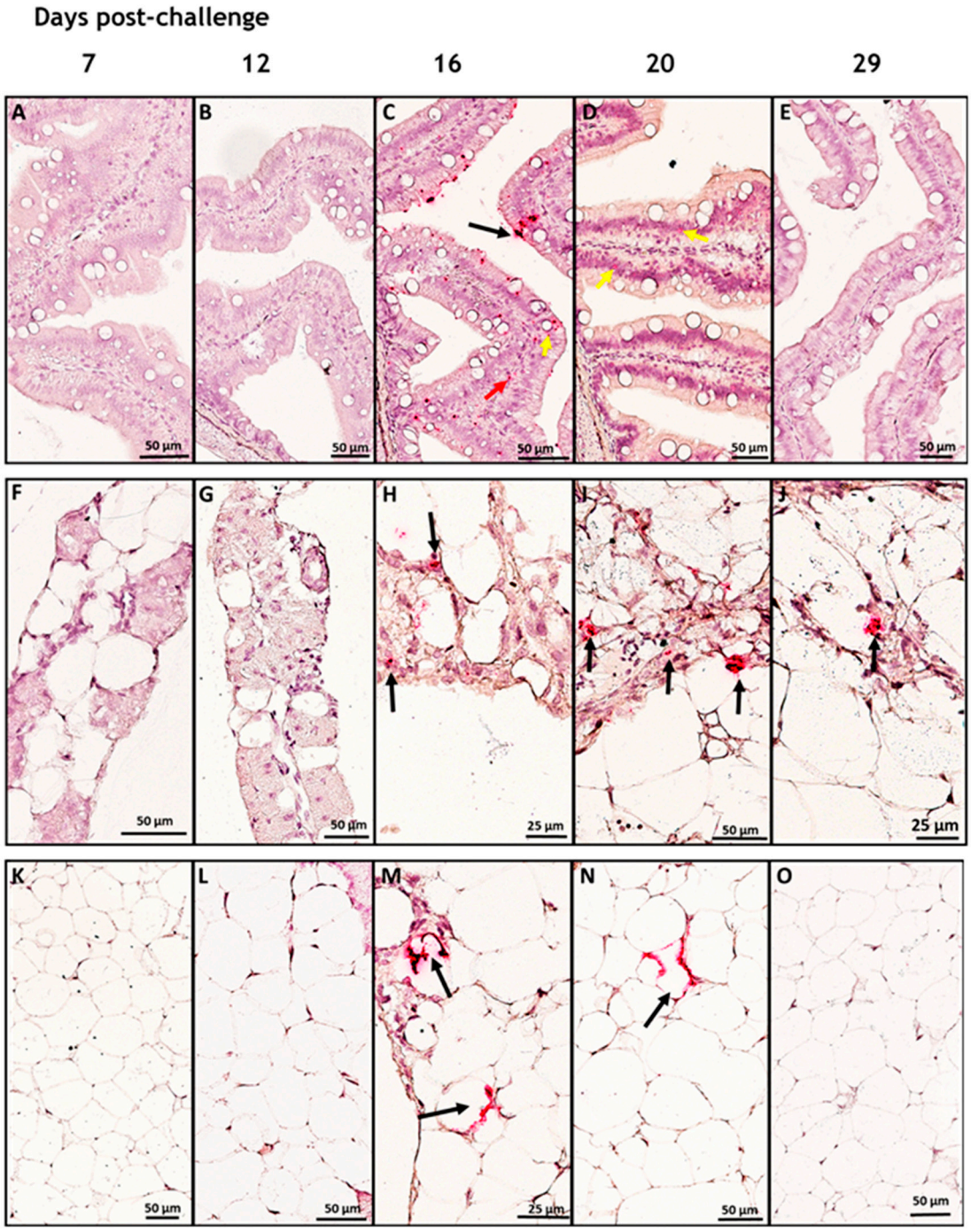

Figure 4. In situ hybridization (RNAscope) of SAV3 in pyloric caeca (A – E), pancreas tissue (F – J), and their associated adipose tissue (K – O) of Atlantic salmon challenged with the virus by the cohabitation method. Tissues collected from fish in the high-dose group at different time points after challenge, showed SAV-specific hybridization signal (red staining and arrows) in the PC at 16 and 20 dpc on the apical part of the villi (probably attached to the mucus; black arrows), in the epithelial columnar cells (yellow arrows), and in cells in the lamina propria (red arrows). SAV-specific staining was also detected in some cells in the pancreas region at 12, 16, and 20 dpc (H, I, and J, respectively) and in the cytoplasm of adipocytes in the associated adipose tissue at 12 and 20 dpc (M and N, respectively).

With the detection of the SAV3 at 20 dpc, the trunk kidney was the tissue with the lowest SAV3 prevalence in the current study. The samples collected at 20 dpc showed a 'humble' SAV3 hybridization staining (Figure 5D). At that time point, the signal seemed to be associated with the cytoplasm of adipocytes in the surrounding adipose tissue (Figure 5F), as well as with a few cells dispersed in the renal parenchyma (Figure 5G).

Preprints (www.preprints.org) | NOT PEER-REVIEWED | Posted: 18 October 2023 doi:10.20944/preprints202310.1132.v1

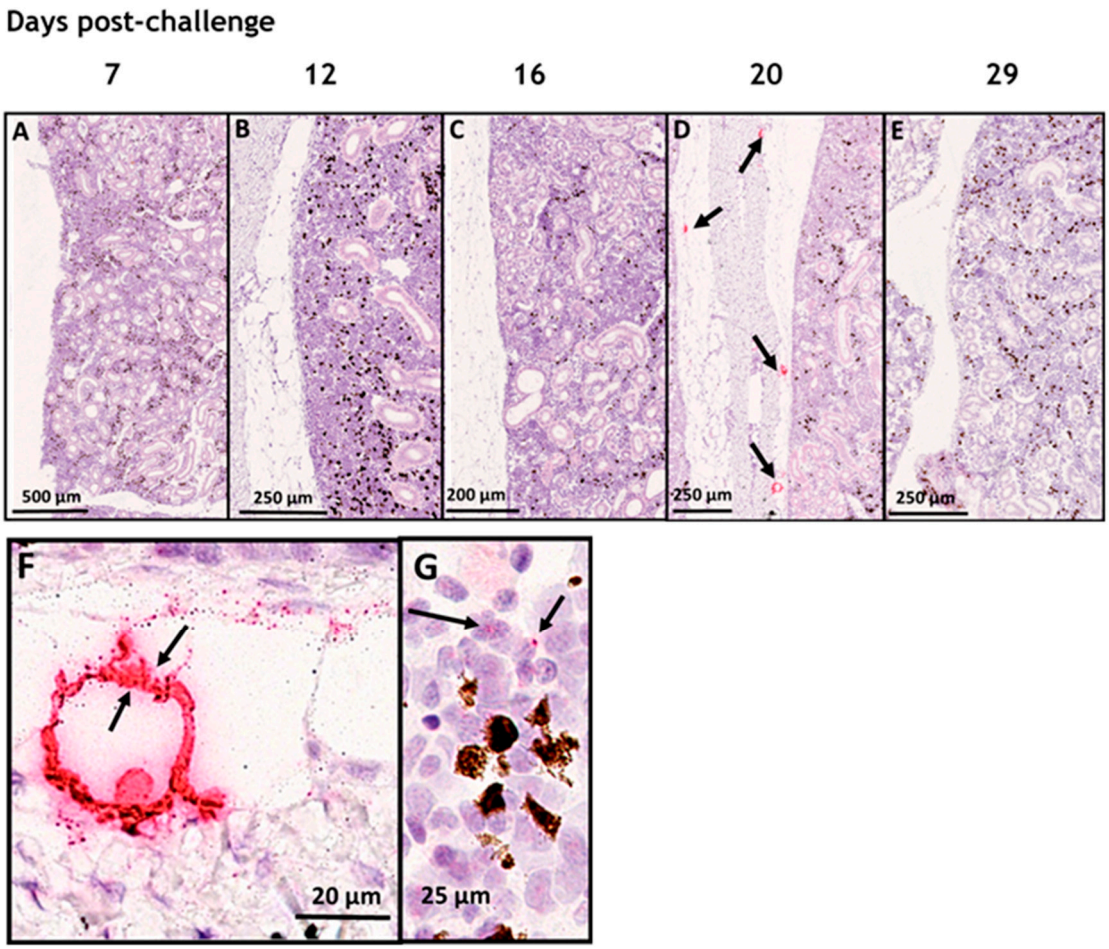

Figure 5. In situ hybridization (RNAscope) of SAV3 in posterior kidney of Atlantic salmon challenged with the virus by the cohabitation method. Posterior kidney tissues collected from fish in the high-dose group at different time points after challenge, showed SAV-specific hybridization signal (red staining and arrows) in ⊛D′. SAV-specific staining detected in ⊛D′ is shown on a higher magnification in (F and G) to show the hybridization associated with the cytoplasm of adipocytes in gills-associate adipose tissue (arrows in ⊛F′) and in association with few cells in the parenchyma (arrows in ⊛G′).

Nevertheless, the other compartments of the trunk kidney, including, proximal and distal tubules, and the renal corpuscle showed no SAV-specific hybridization at any of the time points analyzed. Interestingly, the liver, spleen and its surrounding adipose tissue showed no SAV hybridization at any of the time points (Figure 6A–E), (Figure 6K–M) and (Figure 6F–J), respectively.

Preprints (www.preprints.org) | NOT PEER-REVIEWED | Posted: 18 October 2023 doi:10.20944/preprints202310.1132.v1

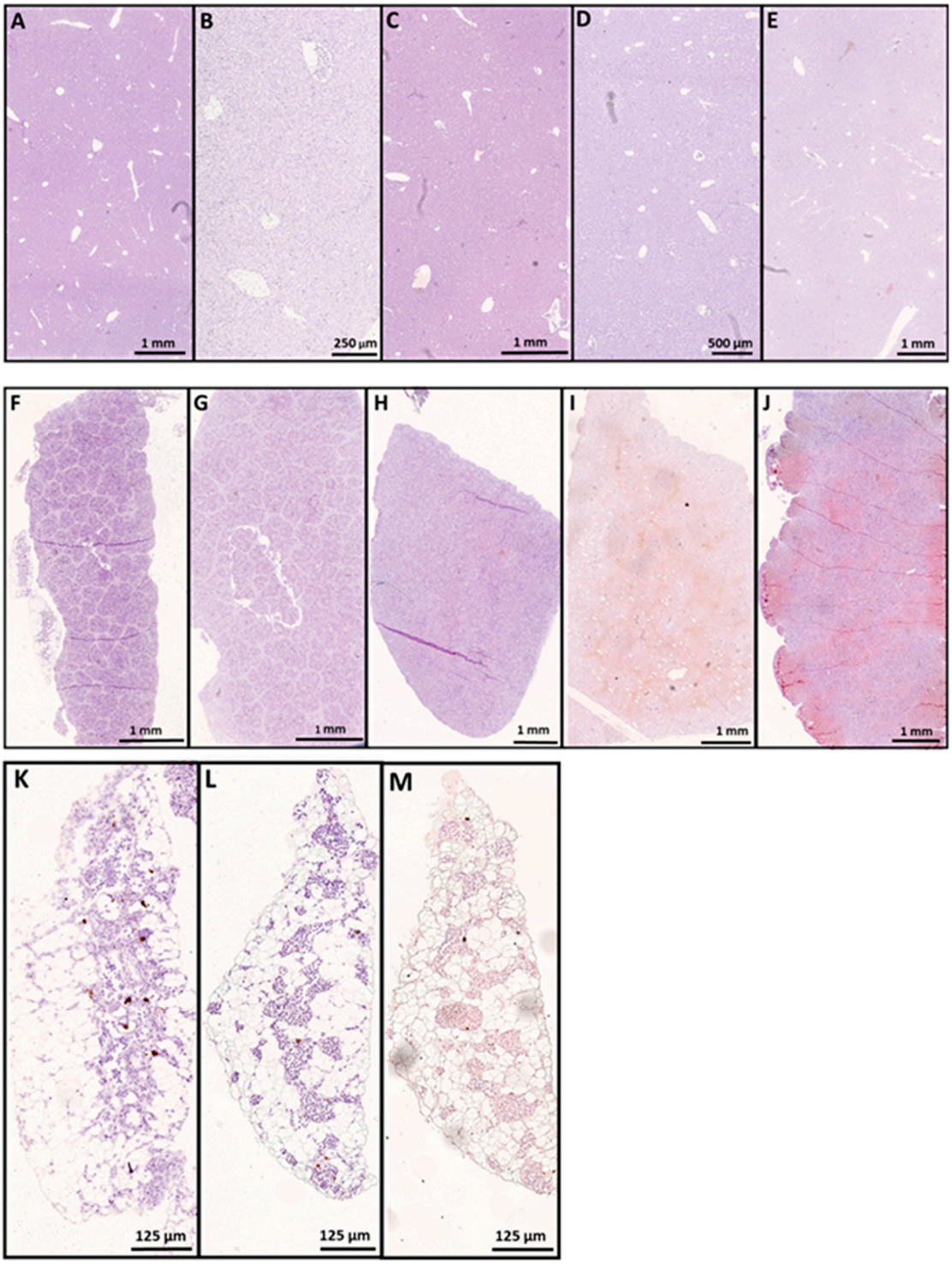

Figure 6. In situ hybridization (RNAscope) of SAV3 in liver (A – E), spleen (F – J) and its associated adipose tissue (K – M) of Atlantic salmon challenged with the virus by the cohabitation method. Tissues collected from fish in the high-dose group at 7 (A, F and K), 12 (B and G), 16 (C and H), 20 (D, I and L) and 29 (E, J and M) dpc, showed no SAV-specific hybridization signal at any of the time points analyzed.

Preprints (www.preprints.org) | NOT PEER-REVIEWED | Posted: 18 October 2023 doi:10.20944/preprints202310.1132.v1

3.2. SAV-nsP1 Quantification

The SAV load in the heart and pseudobranch tissues was studied throughout the challenge period (0 – 29 dpc) by quantifying the expression of *nsP1* gene in both tissues from fish in the LD, HD, and Ctr. tanks using quantitative RT-qPCR and *Q_nsp1* assay. For fish in the control group, no *nsp1* gene expression was detected at any of the time points analyzed (**Figure 7).** Heart and pseudobranch of fish exposed to low and high doses of SAV showed no *nsP1* expression (median Cq value > 44) at 7 dpc. At 12 dpc, fish in the HD group showed higher SAV Cq values than that in the LD group with *nsp1* median Cq values of 31 vs. 45 in the heart and 28 vs. 41 in the pseudobranch, as shown in **Figure 7.** The difference in expression between the LD and HD groups was less pronounced at the later time points. At 16 dpc, for example, while fish in LD and HD groups had comparable levels of *nsp1* expression in the heart (Cq values of 23 and 24, respectively), both groups showed a median Cq value of 27 in the pseudobranch. In the period between 19 and 29 dpc, the median Cq values of *nsp1* in the virus-exposed groups ranged between 16.9 and 22.3, and 22.2 and 34.1 for both heart and pseudobranch, respectively. The virus load remained relatively constant in both heart and pseudobranch tissue samples toward the end of the experiment **(Figure 7).**

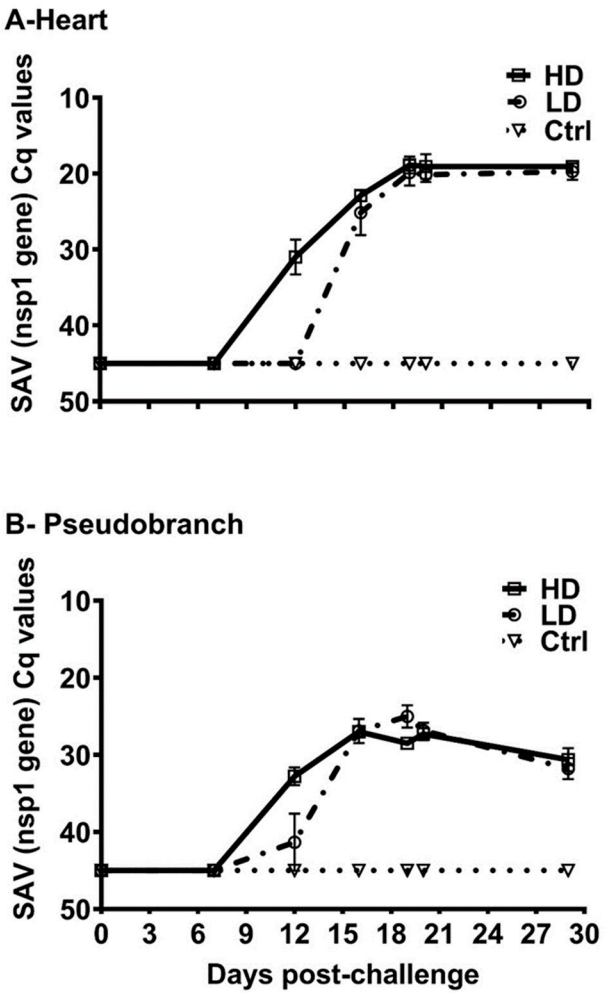

Figure 7. SAV3 infection load in (A) heart and (B) pseudobranch of salmon fish exposed to no (Ctrl; control fish) low (LD) or high (HD) dose of the virus (challenge by cohabitation with virus-shedding fish) from 0 to 29 dpc based on the expression of SAV-*nsp1* gene (Ct values; median with range) using RT-qPCR (Q_nsp1 assay).

3.3. Immune Response in Pseudobranch against SAV

We investigated the immune response in pseudobranch to the challenge with SAV3 by analyzing the expression of genes related to both innate and adaptive immune mechanisms.

 doi:10.20944/preprints202310.1132.v1

3.3.1. Genes Linked to Antiviral Activity

Genes related to the antiviral activity showed a generic upregulation pattern in the pseudobranch in response to SAV exposure. As early as 7 dpc, both LD and HD groups showed high transcript levels of *Mx* gene that were significantly different from that of the control group and which lasted up to 20 dpc (Figure 8). The change in expression of *viperin* and *IFNγ*, on the other hand, showed a late response to virus exposure and was not significant in the SAV3-challenged groups until 16 dpc. Between 16 and 20 dpc, the mRNA of *Viperin* showed a steady high level in the virus-exposed groups (median ≥ 5.5 fold) before it dropped toward the end of the experiment leading to transcript levels only significant in the LD group (Figure 8). The SAV-infected fish in LD and HD groups also showed a generally higher *IFNγ* transcript (median ≥ 3 fold) from 16 dpc and until the end of the experiment with a transient downregulation (median < 3.5 fold), at 19 dpc in both groups (Figure 8). Interestingly, *IFNα* showed a general upregulation throughout the infection course; however, the change was only significant for the LD group at 12 and 20 dpc (Figure 8).

3.3.2. Major Histocompatibility Molecules

The change in *MHC-I* transcript levels was consistent, and a general upregulation with varied fold numbers (median ≥ 0.9) was detected throughout the infection course in both LD and HD groups; however, the expression was not significantly different from that of the control group until 12 dpc (Figure 8). On the other hand, the analysis of the difference in *MHC-II* expression in the pseudobranch between the SAV3-challenged and control fish showed a single transient, yet prominent, significant value in fish in the HD group around the virus peak in the pseudobranch (RT-qPCR) as shown in Figure 8.

3.3.3. Genes Linked to T Cell

The expression patterns of *CD8a* and granzyme A (*gzma*) were almost similar in the pseudobranch of fish exposed to SAV3 (Figure 9). The mRNA levels of both genes were significantly higher (median of 1.5 – 7 folds) in the virus-exposed groups in the period between 12 and 20 dpc (as compared to the control) with an exception at 19 dpc where a significant downregulation of both genes (median ≥ 2.5 folds) was recorded (Figure 9). NK-lysin showed a different pattern of expression from that of *CD8a* and *gzma* (Figure 9). While fish in the LD group had no significant differences from that of the control group along the SAV infection course, fish in the HD group showed a significantly low level (median = 2.5 folds) at 12 dpc and a significantly high level (median = 5 folds) at 20 dpc as compared to both the control and the LD groups (Figure 9). As for the *CD4*, there were no significant differences in the mRNA levels between the SAV3-infected and control fish, except for the lower and higher transcripts in the LD group at 12 and 16 dpc, respectively.

3.3.4. Immunoglobulins

After SAV exposure, genes related to adaptive humoral immune response (immunoglobulin genes) showed a less prominent change as compared to that of genes linked to CD8 T cells or the antiviral activity. For IgM, while the mRNA level of *mIgM* in LD and HD groups showed a single significant upregulation event (median ≥ 3 folds) at 12 dpc, the change in the sIgM was remarkable at a later time (29 dpc; median ≥ 3.5 folds higher in virus-exposed groups), as shown in Figure 9. On the other hand, the expression patterns of *mIgTB* and *sIgTB* in the challenged groups showed no significant differences from that of the control group at any of the time points analyzed (Figure 9).

Preprints (www.preprints.org) | NOT PEER-REVIEWED | Posted: 18 October 2023 doi:10.20944/preprints202310.1132.v1

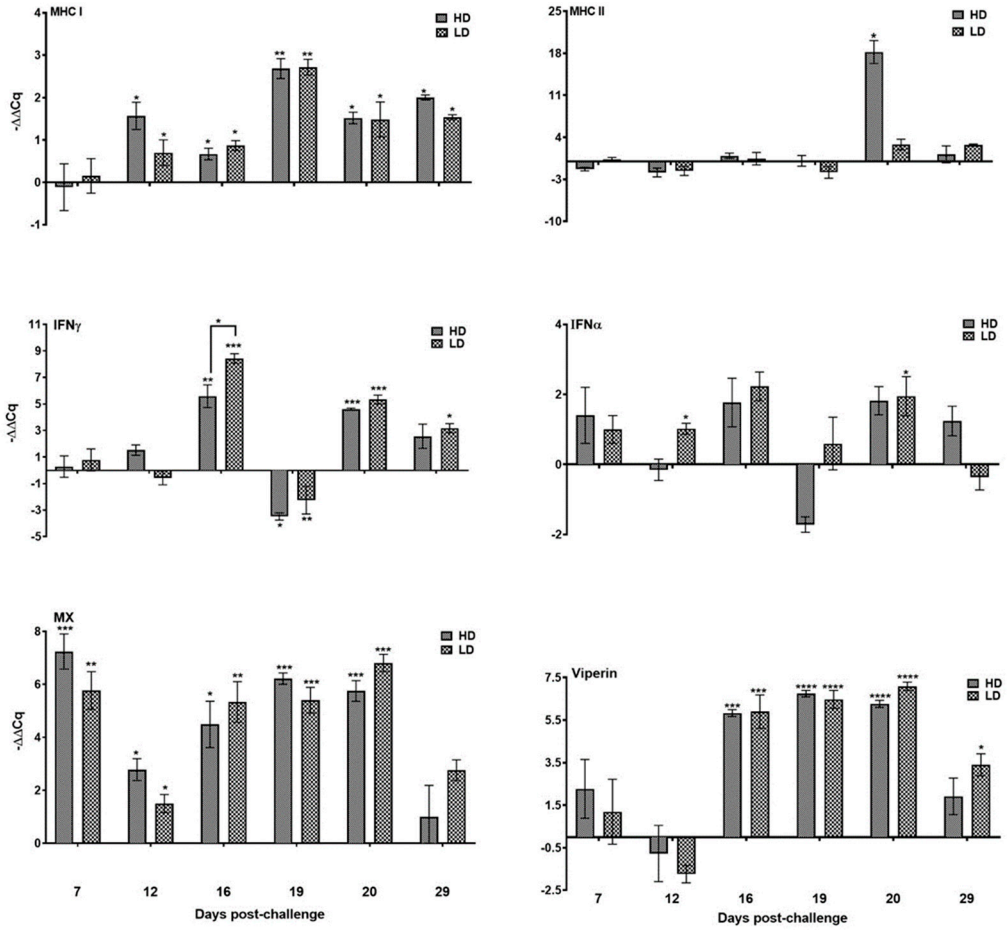

Figure 8. Relative gene expression (median with range) of major histocompatibility complex class I and II (*MHC-I* and *MHC-II*), interferon-alpha (*IFN-α*), interferon-gamma (*IFN-γ*), virus inhibitory protein, endoplasmic reticulum-associated, interferon-inducible (*viperin*), and myxovirus resistance 1 (*Mx*) in the pseudobranch of Atlantic salmon exposed to low (LD) and high (HD) doses of SAV from 0 to 29 dpc. Asterisks above solid lines between groups represent significant changes between the denoted groups and asterisks above the individual groups represent a significant difference between these groups and the non-exposed control fish. *P < 0.05, **P < 0.005, and ***P < 0.0005.

Preprints (www.preprints.org) | NOT PEER-REVIEWED | Posted: 18 October 2023 doi:10.20944/preprints202310.1132.v1

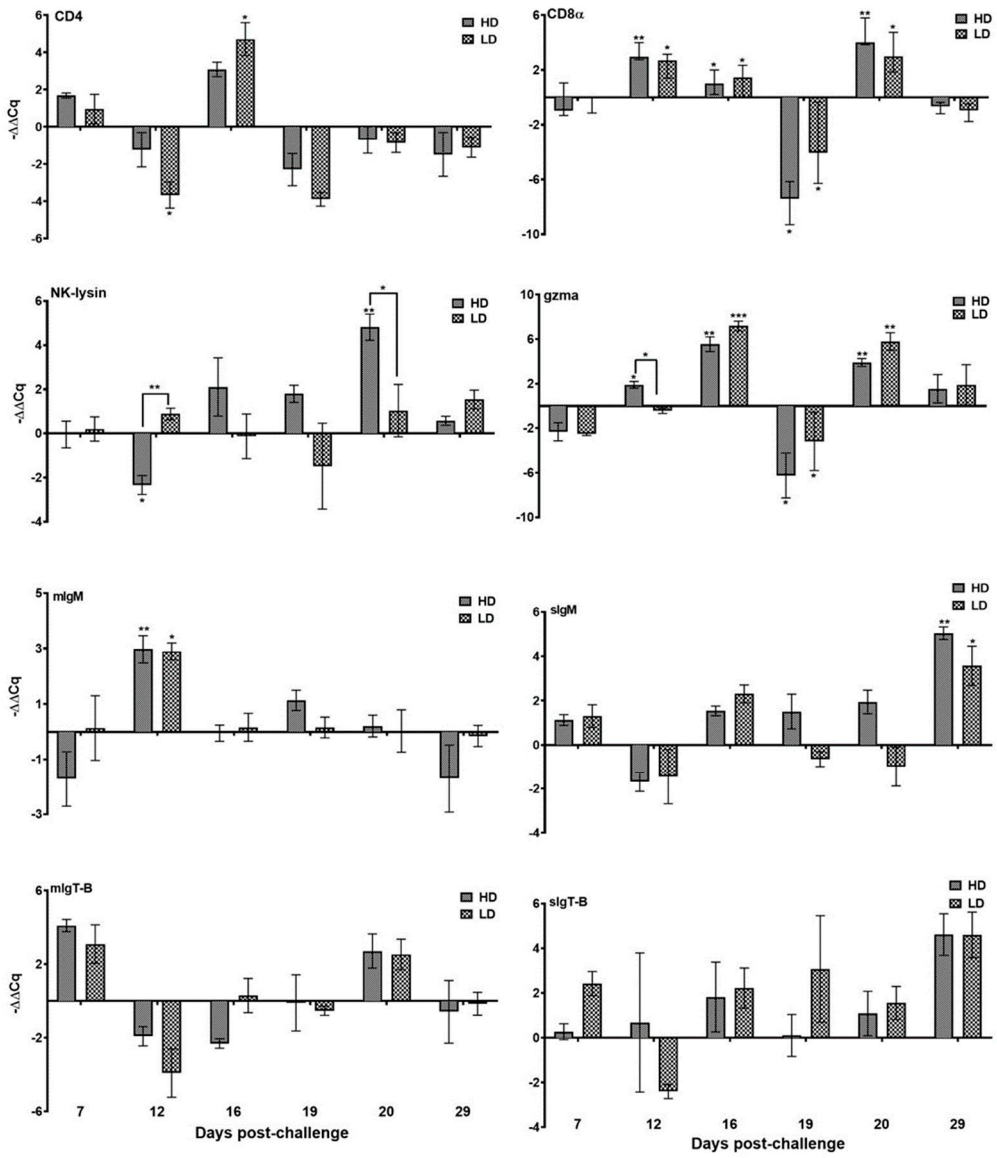

Figure 9. Relative gene expression (median with range) of cluster of differentiation 4 (*CD4*), cluster of differentiation 8 alpha (*CD8a*), granzyme A (*gzma*), natural killer lysin (*NK-lysin*), membrane and secretory immunoglobulin M (*mIgM* and *sIgM*, respectively), and membrane and secretory immunoglobulin T sub-isotype B (*mIgT-B* and *sIgT-B*, respectively) in pseudobranch of Atlantic salmon fish exposed to low (LD) and high (HD) doses of SAV from 0 to 29 dpc. Asterisks above the groups represent the significant difference of the denoted group from the non-exposed control fish. *P < 0.05, **P < 0.005 and ***P< 0.0005.

Preprints (www.preprints.org) | NOT PEER-REVIEWED | Posted: 18 October 2023 doi:10.20944/preprints202310.1132.v1

3.3.5. Mucin Gene Expression

We also studied the change in the mRNA levels of two mucin genes (*Muc-2 and Muc-5*; previously studied in Atlantic salmon gills and showed expression changes upon pathogenic insults [37]) in the pseudobranch after SAV3 exposure. Although the varied mRNA amounts measured throughout the infection trials showed a general tendency of downregulation, the SAV3-infected fish pseudobranch showed no significant difference from the control fish at any of the time points analyzed (Figure 10).

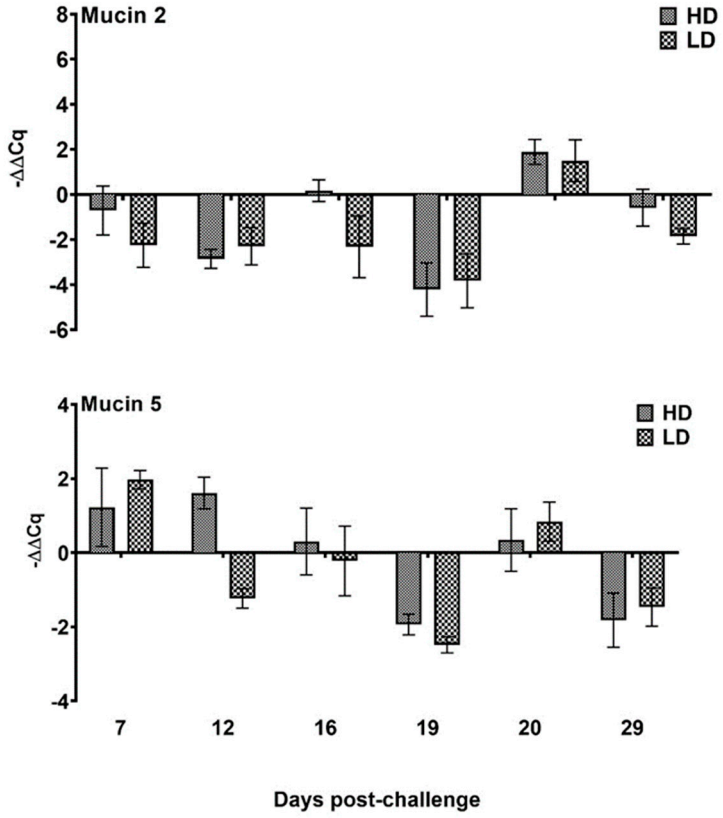

Figure 10. Relative gene expression (median with range) of mucin genes (*Muc-2* and *Muc-5*) in the pseudobranch of Atlantic salmon fish exposed to low (LD) and high (HD) doses of SAV from 0 to 29 dpc showing no significant change at any of the time points analyzed.

4. Discussion

In the current study, an in situ hybridization protocol (RNAscope) was successfully used to detect SAV3 in situ in tissues of the virus-infected salmon and to demonstrate the tropism of the virus during the acute phase of the disease, by employing a challenge model based on cohabitation with virus-shedding fish. In addition, we also described the response of some immune genes to SAV3 infection in the pseudobranch, a tissue that was claimed to harbor the virus for a long time regardless of the state of the disease it causes [11]. Our analyses avoided the dead fish and depended only on fish that had been euthanized at the time of sampling and there could be some samples with different virus distribution and immune response patterns that were not studied.

When the PD was first characterized in salmon, the injection of spleen homogenate from infected fish into healthy individuals could reproduce the infection [39–41], and the virus was suggested to localize in the infected spleen. However, although varied degrees of gross and microscopic changes were detected in the spleen and liver of SAV3-infected fish in natural [42], and experimental [2,43] cases, there was no mention that the virus was detected in these tissues in these studies. In our study, the virus was not detected in the spleen or liver of the SAV3-infected fish, not even around the virus peak. In the posterior kidney also, the virus was detected in a few cells dispersed in the renal parenchyma, and was absent in the excretory compartments. Given that SAV3 can be detected in the

 doi:10.20944/preprints202310.1132.v1

blood of the virus-infected fish during the acute phase of infection [44], the ill detection of the virus in the well-perfused tissues in our study becomes interesting. Indeed, the time interval of the acute phase of SA3 infection (when the viremia is to be expected) in a previous challenge trial was estimated to be 3 – 5 weeks post-challenge [2]. However, in that study, the virus was introduced to the fish through the i.p. route with an expected higher infection load and quicker dissemination to the blood than in our cohabitation model.

Despite these differences, similar findings between the different challenges were also observed. For example, the time of the detection of SAV3 RNA in a few cells in the pancreas rergion between 16 – 29 dpc in our model agreed with the significant detection of the virus in the pancreatic tissue 21 – 37 days post-injection in the i.p. challenge model [2]. However, in that study, the pancreas had the lowest prevalence of SAV3 RNA among the other salmon tissues and was proposed to be an unsuitable tissue for PD diagnosis using RT-PCR. In addition, the pancreas samples analyzed in that study were combined with the pyloric caeca sample and do not necessarily represent the pancreas results exclusively. In our challenge model, the virus detection in the pyloric caeca was confirmed at 16 and 20 dpc in association with the cells wandering in the lamina propria of the intestinal mucosa, and also in columnar epithelial cells and the covering mucus layer. These results agree with the previous findings showing SAV-infected fish to shed the virus in faeces during experimental challenge[45].

Also in their tropism study, Andersen et al., [2] showed that the pseudobranch and heart ventricle had the highest prevalence of viral RNA regardless of the PD status. In our results, both tissues showed a consistent detection of SAV3 in the infected fish from the time of the virus peak until the end of the experiment (RNAscope and RT-qPCR data). Nevertheless, although the RNAscope data showed no SAV detection before 16 dpc, the early onset of the ‘humble’ detection of the virus (Cq = 37) in the pseudobranch of fish before the heart in the LD group, using the highly sensitive Q_nsp1 assay, can suggest the SAV kinetic direction between the two tissues to be from outward (pseudobranch) to inward (heart). Indeed, the detection of SAV in the pseudobranch of salmonids [2] and non-salmonid fish [19] in the virus challenge experiments, affirms the importance of that tissue for SAV pathogenicity. However, that potential role in pathogenicity was not necessarily accompanied with SAV-specific histological alterations in the pseudobranch, in contrast to the significant heart lesions (both data not shown), confirming the similar previous results of Christie et al. [7]. The difference in histopathology between the two tissues can probably be attributed to, among many other factors, the higher virus load in the heart as compared to the pseudobranch. Although this line of argument can be supported with the previous results showing the severity of PD pathology in salmon to correlate positively with the virus amount [31], it is still interesting that other tissues with decent SAV amounts (e.g. liver) can show pathological alterations in SAV-infected fish [2,19].

Besides the virus detection in the lamellae of the pseudobranch, the virus was also detected in the tissue-associated adipocytes. Indeed, there was a consistent pattern of detecting SAV in the organs-associated adipose tissue in salmon. An observation that suggests a virus-specific affinity to one or more of the components in the salmon adipocytes. Viable SAV particles were identified in the lipid fraction leaking from the dead PD-infected salmon and was proposed to contribute to the horizontal transmission of the virus, at least in vitro[46]. A significant amount of literature also showed the susceptibility of mammalian adipocytes to different viruses, including for example, Ebola [47] and Covid-19 virus [48], and several laboratory studies reported that alphaviruses’ infections in obese mice were more severe as compared to healthy-weight animals [49]. The fact that adipocytes differentiate from fibroblasts [50] (known target cells for alphavirus replication [51]) makes them also a potential candidate for alphavirus propagation. Interestingly, the adipose tissue associated with the spleen showed no SAV detection, probably due to a difference in the cellular and/or molecular components between the different adipose tissue sites.

Despite the SAV detection in the adipose tissues associated with both the pseudobranch and the gill tissues, the virus detected in the functional compartment of the gills (i.e. lamella) was less prominent than that of the pseudobranch. An observation that agrees to a certain extent with that the pseudobranch can have a SAV3 prevalence percentage higher than that of the gills in virus-challenged fish up to 91 dpc [2]. The low prevalence of SAV in gills can be linked to the pathogen clearance ability of the gills exerted by their continuously secreted mucus [52]. Such a feature has not been confirmed

 doi:10.20944/preprints202310.1132.v1

yet in the salmon pseudobranch, considering its deeply buried nature, the opercula tissue, and its fused lamellae, with no contact with the aquatic milieu [13] or expectation of mucus secretion. An argument that can be supported at least by our results showing no change in the low mRNA levels of two mucin genes (*Muc-2* and *Muc-5*) in the pseudobranch of SAV3-infected fish. Despite the potential difference, both the gills and pseudobranch tissues were stated in the previous literature to harbor SAV for a long time without a noticeable pathological damage [53].

That said, the change in the immune components of the pseudobranch in response to the persistent infection was interesting to investigate. Among the innate immune genes regulated in the pseudobranch after SAV exposure, *Mx* was the earliest and the most consistent throughout the infection course. Mx proteins are known for their antiviral activities in different species[54], with either an interferon-dependent [55] or independent [56] induction mechanism in different viral infections. The latter kind of induction is more likely the one responsible for the early upregulation of *Mx* in the current study since it was noticed regardless of the regulation state of *IFN* genes. However, a positive correlation was established between the IFN-dependent stimulation of Mx and the protection against SAV-induced cytopathogenic effects in vitro [57,58] , and hence the efficacy of the response becomes questionable. The expression of the other antiviral genes in the current study (*viperin*) seemed to be *IFN*-dependent, showing late upregulation that coincided with the upregulation of *IFN-γ* around the virus peak. In mammals, interferons (including *IFNα*, *IFNβ*, *IFNγ*) can induce an antiviral state in vertebrate cells [59]. In the current study, the absence of a consistent increase in *IFN-α* in the SAV-infected pseudobranch along the infection course can suggest a reduced antiviral activity against the virus, probably contributing to the persistent infection of the SAV in that tissue. On the other hand, the increase in *IFN-γ* around the virus peak does not necessarily mean efficient protection against SAV, considering the results of the *in vitro* infection model showing rIFN-γ to have a mild antiviral activity against SAV3 [60]. In all cases, the early initiation of the IFN system as part of the host innate immune response in salmon was considered important for protection against SAV3 [61].

On the other hand, genes related to the adaptive immune response showed a modest change upon SAV3 infection. The response of the two T cell co-receptors (CD4 and CD8; which enhance the recognition of the MHC–peptide complex by the T cell receptor and hence the T cell activation [62]) to SAV infection varied. We confirmed an increase in the transcription of cytotoxic T-cell marker (*CD8a*) and its killing mediator (*gzma*) in SAV-infected pseudobranch. Both molecules are associated with adaptive immune cytotoxic T-cells and are involved in intracellular antigen recognition and cell-mediated killing, respectively, and their increase in response to SAV infection is probably to clear the virus-infected cells. The consistent upregulation of the *CD8a*, and *gzma*, as well as, *MHC-I* in the pseudobranch of SAV3-infected fish is an indication of mounting a Th1 cytotoxic immune response against SAV, supporting a previous proposal of the implication of the adaptive cell-mediated immunity in SAV-infected salmon in the in vivo infection model [61]. Accordingly, the upregulated *MHC-II* (expressed by the professional antigen-presenting cells; APCs [63]) at a later time point suggests kinetics of the APCs in pseudobranch in response to the exogenous virus material released from the SAV-infected cells cleared by the Th1 mounted response. As the presentation of pathogen-derived antigens by *MHC-II* on the APCs' surfaces is essential to the elicitation of CD4 T cell binding [63], a simultaneous increase in the *CD4* expression (due to CD4 cell kinetics) should have been detected. Interestingly, this was not the case where the only *CD4* upregulation event was identified around the virus peak. With the discontinuation of T cell responses toward the end of the trial, an insufficient activity against SAV can be anticipated.

The upregulation of *mIgM* around the virus peak in the pseudobranch, suggests the kinetics of B cells in response to the infection. A reaction that can be seen as part of the B cell conserved antigen recognition and processing [64], even earlier than the other professional APCs (as judged by late expression of *MHC-II*). If not for the unchanged expression of *MHC- II*, the synchronized upregulation of *CD4* and *mIgM* (hence the kinetics of T helper and B cells, respectively) early during the infection could have been related to the late upregulation of *sIgM*. However, a T cell-independent activation of B cells, previously studied in vesicular stomatitis virus [65], can be suggested to be responsible for the late increase in *sIgM*. The upregulation of *sIgM* can indicate a possibility of producing SAV3-specific antibody. This suggestion can be supported by the results showing the detection of SAV-specific antibodies in the plasma of SAV-challenged fish at 3 – 6 weeks post-

challenge [66]. Interestingly, the *IgT* pattern of expression was different from that of the IgM, where no response was detected. Indeed, the mucosal tissue is the main compartment of teleosts' IgT isotype [67], a feature that has not been used to describe the salmon pseudobranch, so far. With the no change pattern in *IgT* expression, the importance of that isotype for the salmon pseudobranch is probably trivial.

5. Conclusions

We managed to use an *in situ* hybridization protocol (RNAscope®) to detect SAV3 in situ in tissues of the virus-infected salmon and demonstrated the tropism of the virus during the acute phase of the experimental cohabitation infection. While no SAV3 was detected in the spleen or liver, the heart, gills, pseudobranch, pyloric caeca, posterior kidney and pancreas showed varried levels of detection. Interestingly, we also demonstrated a ubiquitous identification of the virus in the adipose tissue distributed around the different internal organs in salmon, except for that around the spleen. The persistent low infection of the virus in the pseudobranch along with the inconsistent immune response to SAV3 infection can suggest a pivotal role of the pseudobranch in SAV3 pathogenesis in Atlantic salmon.

Author Contributions: "Conceptualization, H.T., L.V.B., and S.C.W.; methodology, H.T., S.N.M., L.V.B., S.C.W. and R.K., ; software, R.K., L.V.B., and H.T.; validation, R.K., L.V.B., and H.T.; S.C.W. and S.N.M.; formal analysis, H.T., R.K., and S.C.W.; investigation, H.T., L.V.B., R.K., and S.C.W.; resources, S.C.W.; data curation, H.T., L.V.B., R.K., S.N.M., and S.C.W.; writing—original draft preparation, H.T., and S.C.W.; writing—review and editing, R.K., L.V.B., H.T., S.N.M., and S.C.W.; visualization, H.T., R.K., and S.C.W.; supervision, S.W.; project administration S.C.W.; funding acquisition, S.C.W. All authors have read and agreed to the published version of the manuscript."

Funding: This research was funded by the Research Council of Norway, grant number 267411 and The Norwegian Ministry of Trade, Industry, and Fishery: Biosecurity in Aquaculture grant 13055.

Institutional Review Board Statement: The current study was approved by the Norwegian Food safety Authority (FOTS :).

Data Availability Statement: The data presented in this study are available on request from the corresponding author. The data are not publicly available as it is a part of an application that is to be submitted to FRIPRO https://www.forskningsradet.no/portefoljer/banebrytende-forskning/.

Acknowledgments: We thank Linda Andersen and Steffen H. Blindheim at the Industrial and Aquatic Laboratory (ILAB, Bergen) for providing facilities and for their support during this challenge; Hilde Sindre for providing the SAV3 isolate and colleagues at the section for Pathology at Norwegian Veterinary Institute, Ås for preparing and staining histological sections. Lisa-Victoria Bernhardt was affiliated with the Norwegian Veterinary Institute at the time of the trial and is currently affiliated with the Group Research and Development at DNV.

Conflicts of Interest: The authors declare no conflict of interest and the funders had no role in the design of the study; in the collection, analyses, or interpretation of data; in the writing of the manuscript; or in the decision to publish the results.

References

1. Peters, C.J.; Dalrymple, J.M. Alphaviruses; ARMY MEDICAL RESEARCH INST OF INFECTIOUS DISEASES FORT DETRICK MD: 1990.
2. Andersen, L.; Bratland, A.; Hodneland, K.; Nylund, A. Tissue tropism of salmonid alphaviruses (subtypes SAV1 and SAV3) in experimentally challenged Atlantic salmon (Salmo salar L.). Archives of virology 2007, 152, 1871-1883.
3. Nelson, R.; McLoughlin, M.; Rowley, H.; Platten, M.; McCormick, J. Isolation of a toga-like virus from farmed Atlantic salmon Salmo salar with pancreas disease. Diseases of aquatic organisms 1995, 22, 25-32.
4. Castric, J.; Baudin Laurencin, F.; Bremont, M.; Jeffroy, J.; Ven, A.l.; Bearzotti, M. Isolation of the virus responsible for sleeping disease in experimentally infected rainbow trout (Oncorhynchus mykiss). Bulletin of the European Association of Fish Pathologists 1997, 17, 27-30.
5. Graham, D.; Rowley, H.; Walker, I.; Weston, J.; Branson, E.; Todd, D. First isolation of sleeping disease virus from rainbow trout, Oncorhynchus mykiss (Walbaum), in the United Kingdom. Journal of fish diseases 2003, 26, 691-694.

6. Christie, K.; Fyrand, K.; Holtet, L.; Rowley, H. Isolation of pancreas disease virus from farmed Atlantic salmon, Salmo salar L., in Norway. Journal of Fish Diseases 1998, 21, 391-394.
7. Christie, K.; Graham, D.; McLoughlin, M.; Villoing, S.; Todd, D.; Knappskog, D. Experimental infection of Atlantic salmon Salmo salar pre-smolts by ip injection with new Irish and Norwegian salmonid alphavirus (SAV) isolates: a comparative study. Diseases of aquatic organisms 2007, 75, 13-22.
8. Jenberie, S.; Peñaranda, M.M.D.; Thim, H.L.; Styrvold, M.B.; Strandskog, G.; Jørgensen, J.B.; Jensen, I. Salmonid alphavirus subtype 3 induces prolonged local B cell responses in Atlantic salmon (Salmo salar) after intraperitoneal infection. Frontiers in immunology 2020, 11, 1682.
9. Bakke, A.F.; Bjørgen, H.; Koppang, E.O.; Frost, P.; Afanasyev, S.; Boysen, P.; Krasnov, A.; Lund, H. IgM+ and IgT+ B cell traffic to the heart during SAV infection in Atlantic salmon. Vaccines 2020, 8, 493.
10. Moore, L.; Jarungsriapisit, J.; Nilsen, T.; Stefansson, S.; Taranger, G.; Secombes, C.; Morton, H.; Patel, S. Immune gene profiles in Atlantic salmon (salmo salar L.) post-smolts infected with SAV3 by bath-challenge show a delayed response and lower levels of gene transcription compared to injected fish. Fish & Shellfish Immunology 2017, 62, 320-331.
11. Hodneland, K.; Scientiarum, D. SALMONID ALPHAVIRUS (SAV).
12. Parry, G.; Holliday, F. An experimental analysis of the function of the pseudobranch in teleosts. Journal of Experimental Biology 1960, 37, 344-354.
13. Waser, W. Transport and exchange of respiratory gases in the blood| root effect: root effect definition, functional role in oxygen delivery to the eye and swimbladder. 2011.
14. Grassé, P.-P. Traité de zoologie: Agnathes et poissons; Masson: 1958.
15. Barnett, C. The structure and function of the choroidal gland of teleostean fish. Journal of anatomy 1951, 85, 113.
16. Karlsbakk, E.; Sæther, P.; Hostlund, C.; Fjellsoy, K.; Nylund, A. Parvicapsula pseudobranchicola n. sp.(Myxozoa), a myxosporidian infecting the pseudobranch of cultured Atlantic salmon (Salma salar) in Norway. BULLETIN-EUROPEAN ASSOCIATION OF FISH PATHOLOGISTS 2002, 22, 381-387.
17. Valheim, M.; Håstein, T.; Myhr, E.; Speilberg, L.; Ferguson, H.W. Varracalbmi: a new bacterial panophthalmitis in farmed Atlantic salmon, Salmo salar L. Journal of Fish Diseases 2000, 23, 61-70.
18. Hauck, A. A mortality and associated tissue reactions of chinook salmon, Oncorhynchus tshawytscha (Walbaum), caused by the microsporidan Loma sp. Journal of Fish Diseases 1984, 7, 217-229.
19. Andersen, L.; Blindheim, S.H. Experimental challenge of flatfishes (Pleuronectidae) with salmonid alphavirus (SAV): Observations on tissue tropism and pathology in common dab Limanda limanda L. Aquaculture 2022, 551, 737944.
20. Bernhardt, L.-V.; Myrmel, M.; Lillehaug, A.; Qviller, L.; Weli, S.C. Concentration and detection of salmonid alphavirus in seawater during a post-smolt salmon (Salmo salar) cohabitant challenge. Diseases of Aquatic Organisms 2021, 144, 61-73.
21. Andersen, L.; Hodneland, K.; Nylund, A. No influence of oxygen levels on pathogenesis and virus shedding in Salmonid alphavirus (SAV)-challenged Atlantic salmon (Salmo salar L.). Virology journal 2010, 7, 1-14.
22. Reed, L.J.; Muench, H. A simple method of estimating fifty per cent endpoints. American journal of epidemiology 1938, 27, 493-497.
23. Hodneland, K.; Endresen, C. Sensitive and specific detection of Salmonid alphavirus using real-time PCR (TaqMan®). Journal of virological methods 2006, 131, 184-192.
24. Ingerslev, H.-C.; Pettersen, E.F.; Jakobsen, R.A.; Petersen, C.B.; Wergeland, H.I. Expression profiling and validation of reference gene candidates in immune relevant tissues and cells from Atlantic salmon (Salmo salar L.). Molecular immunology 2006, 43, 1194-1201.
25. Livak, K.J.; Schmittgen, T.D. Analysis of relative gene expression data using real-time quantitative PCR and the 2− ΔΔCT method. methods 2001, 25, 402-408.
26. Kileng, Ø.; Brundtland, M.I.; Robertsen, B. Infectious salmon anemia virus is a powerful inducer of key genes of the type I interferon system of Atlantic salmon, but is not inhibited by interferon. Fish & shellfish immunology 2007, 23, 378-389.
27. Ingerslev, H.C.; Rønneseth, A.; Pettersen, E.; Wergeland, H. Differential expression of immune genes in Atlantic salmon (Salmo salar L.) challenged intraperitoneally or by cohabitation with IPNV. Scandinavian Journal of Immunology 2009, 69, 90-98.

28. Grove, S.; Austbø, L.; Hodneland, K.; Frost, P.; Løvoll, M.; McLoughlin, M.; Thim, H.L.; Braaen, S.; König, M.; Syed, M. Immune parameters correlating with reduced susceptibility to pancreas disease in experimentally challenged Atlantic salmon (Salmo salar). Fish & shellfish immunology 2013, 34, 789-798.
29. Kileng, Ø.; Albuquerque, A.; Robertsen, B. Induction of interferon system genes in Atlantic salmon by the imidazoquinoline S-27609, a ligand for Toll-like receptor 7. Fish & shellfish immunology 2008, 24, 514-522.
30. Kumari, J.; Bøgwald, J.; Dalmo, R.A. Eomesodermin of Atlantic salmon: an important regulator of cytolytic gene and interferon gamma expression in spleen lymphocytes. PLoS One 2013, 8, e55893.
31. Braden, L.M.; Rasmussen, K.J.; Purcell, S.L.; Ellis, L.; Mahony, A.; Cho, S.; Whyte, S.K.; Jones, S.R.; Fast, M.D. Acquired protective immunity in Atlantic salmon Salmo salar against the myxozoan Kudoa thyrsites involves induction of MHIIβ+ CD83+ antigen-presenting cells. Infection and immunity 2018, 86.
32. Moldal, T.; Løkka, G.; Wiik-Nielsen, J.; Austbø, L.; Torstensen, B.E.; Rosenlund, G.; Dale, O.B.; Kaldhusdal, M.; Koppang, E.O. Substitution of dietary fish oil with plant oils is associated with shortened mid intestinal folds in Atlantic salmon (Salmo salar). BMC veterinary research 2014, 10, 1-13.
33. Fish, T. Phenotypic and Functional Similarity of Gut. J Immunol 2006, 176, 3942-3949.
34. Strandskog, G.; Villoing, S.; Iliev, D.B.; Thim, H.L.; Christie, K.E.; Jørgensen, J.B. Formulations combining CpG containing oliogonucleotides and poly I: C enhance the magnitude of immune responses and protection against pancreas disease in Atlantic salmon. Developmental & Comparative Immunology 2011, 35, 1116-1127.
35. Wiik-Nielsen, J.; Løvoll, M.; Fritsvold, C.; Kristoffersen, A.B.; Haugland, Ø.; Hordvik, I.; Aamelfot, M.; Jirillo, E.; Koppang, E.O.; Grove, S. Characterization of myocardial lesions associated with cardiomyopathy syndrome in A tlantic salmon, S almo salar L., using laser capture microdissection. Journal of Fish Diseases 2012, 35, 907-916.
36. Lauscher, A.; Krossøy, B.; Frost, P.; Grove, S.; König, M.; Bohlin, J.; Falk, K.; Austbø, L.; Rimstad, E. Immune responses in Atlantic salmon (Salmo salar) following protective vaccination against infectious salmon anemia (ISA) and subsequent ISA virus infection. Vaccine 2011, 29, 6392-6401.
37. Marcos-López, M.; Calduch-Giner, J.A.; Mirimin, L.; MacCarthy, E.; Rodger, H.D.; O'Connor, I.; Sitjà-Bobadilla, A.; Pérez-Sánchez, J.; Piazzon, M.C. Gene expression analysis of Atlantic salmon gills reveals mucin 5 and interleukin 4/13 as key molecules during amoebic gill disease. Scientific reports 2018, 8, 1-15.
38. Moore, L.; Somamoto, T.; Lie, K.; Dijkstra, J.; Hordvik, I. Characterisation of salmon and trout CD8α and CD8β. Molecular immunology 2005, 42, 1225-1234.
39. Raynard, R.; Houghton, G. Development towards an experimental protocol for the transmission of pancreas disease of Atlantic salmon Salmo salar. Diseases of Aquatic Organisms 1993, 15, 123-128.
40. McVicar, A. Infection as a primary cause of pancreas disease in farmed Atlantic salmon. Bulletin of the European Association of Fish Pathologists 1990, 10, 84-87.
41. Houghton, G. Kinetics of infection of plasma, blood leucocytes and lymphoid tissue from Atlantic salmon Salmo salar experimentally infected with pancreas disease. Diseases of Aquatic Organisms 1995, 22, 193-198.
42. Jansen, M.; Wasmuth, M.; Olsen, A.; Gjerset, B.; Modahl, I.; Breck, O.; Haldorsen, R.; Hjelmeland, R.; Taksdal, T. Pancreas disease (PD) in sea-reared Atlantic salmon, Salmo salar L., in Norway; a prospective, longitudinal study of disease development and agreement between diagnostic test results. Journal of fish diseases 2010, 33, 723-736.
43. Taksdal, T.; Bang Jensen, B.; Böckerman, I.; McLoughlin, M.; Hjortaas, M.; Ramstad, A.; Sindre, H. Mortality and weight loss of Atlantic salmon, Salmon salar L., experimentally infected with salmonid alphavirus subtype 2 and subtype 3 isolates from Norway. Journal of fish diseases 2015, 38, 1047-1061.
44. Jarungsriapisit, J.; Moore, L.; Taranger, G.L.; Nilsen, T.; Morton, H.C.; Fiksdal, I.U.; Stefansson, S.; Fjelldal, P.G.; Evensen, Ø.; Patel, S. Atlantic salmon (Salmo salar L.) post-smolts challenged two or nine weeks after seawater-transfer show differences in their susceptibility to salmonid alphavirus subtype 3 (SAV3). Virology journal 2016, 13, 1-14.
45. Graham, D.; Brown, A.; Savage, P.; Frost, P. Detection of salmon pancreas disease virus in the faeces and mucus of A tlantic s almon, S almo salar L., by real-time RT-PCR and cell culture following experimental challenge. Journal of fish diseases 2012, 35, 949-951.
46. Stene, A.; Hellebø, A.; Viljugrein, H.; Solevåg, S.; Devold, M.; Aspehaug, V. Liquid fat, a potential abiotic vector for horizontal transmission of salmonid alphavirus? Journal of fish diseases 2016, 39, 531-537.

47. Gourronc, F.A.; Rebagliati, M.R.; Kramer-Riesberg, B.; Fleck, A.M.; Patten, J.J.; Geohegan-Barek, K.; Messingham, K.N.; Davey, R.A.; Maury, W.; Klingelhutz, A.J. Adipocytes are susceptible to Ebola Virus infection. Virology 2022, 573, 12-22.
48. Thangavel, H.; Dhanyalayam, D.; Lizardo, K.; Oswal, N.; Dolgov, E.; Perlin, D.S.; Nagajyothi, J.F. Susceptibility of Fat Tissue to SARS-CoV-2 Infection in Female hACE2 Mouse Model. International Journal of Molecular Sciences 2023, 24, 1314.
49. Chuong, C.; Bates, T.A.; Akter, S.; Werre, S.R.; LeRoith, T.; Weger-Lucarelli, J. Nutritional status impacts dengue virus infection in mice. BMC biology 2020, 18, 1-14.
50. Tontonoz, P.; Hu, E.; Spiegelman, B.M. Stimulation of adipogenesis in fibroblasts by PPARγ2, a lipid-activated transcription factor. Cell 1994, 79, 1147-1156.
51. Couderc, T.; Chrétien, F.; Schilte, C.; Disson, O.; Brigitte, M.; Guivel-Benhassine, F.; Touret, Y.; Barau, G.; Cayet, N.; Schuffenecker, I. A mouse model for Chikungunya: young age and inefficient type-I interferon signaling are risk factors for severe disease. PLoS pathogens 2008, 4, e29.
52. Thomsson, K.A.; Benktander, J.; Quintana-Hayashi, M.P.; Sharba, S.; Lindén, S.K. Mucin O-glycosylation and pathogen binding ability differ between rainbow trout epithelial sites. Fish & Shellfish Immunology 2022, 131, 349-357.
53. Herath, T.K.; Ferguson, H.W.; Weidmann, M.W.; Bron, J.E.; Thompson, K.D.; Adams, A.; Muir, K.F.; Richards, R.H. Pathogenesis of experimental salmonid alphavirus infection in vivo: an ultrastructural insight. Veterinary research 2016, 47, 1-11.
54. Verhelst, J.; Hulpiau, P.; Saelens, X. Mx proteins: antiviral gatekeepers that restrain the uninvited. Microbiology and Molecular Biology Reviews 2013, 77, 551-566.
55. Kochs, G.; Haller, O. Mx Proteins: High Molecular Weight GTPases with Antiviral Activity. In Handbook of Cell Signaling, Elsevier: 2010; pp. 1855-1864.
56. Ashley, C.L.; Abendroth, A.; McSharry, B.P.; Slobedman, B. Interferon-independent innate responses to cytomegalovirus. Frontiers in immunology 2019, 10, 2751.
57. Lester, K.; Hall, M.; Urquhart, K.; Gahlawat, S.; Collet, B. Development of an in vitro system to measure the sensitivity to the antiviral Mx protein of fish viruses. Journal of virological methods 2012, 182, 1-8.
58. Gahlawat, S.K.; Ellis, A.E.; Collet, B. Expression of interferon and interferon–Induced genes in Atlantic salmon Salmo salar cell lines SHK-1 and TO following infection with Salmon AlphaVirus SAV. Fish & shellfish immunology 2009, 26, 672-675.
59. Verrier, E.R.; Langevin, C.; Benmansour, A.; Boudinot, P. Early antiviral response and virus-induced genes in fish. Developmental & Comparative Immunology 2011, 35, 1204-1214.
60. Xu, C.; Guo, T.-C.; Mutoloki, S.; Haugland, Ø.; Marjara, I.S.; Evensen, Ø. Alpha interferon and not gamma interferon inhibits salmonid alphavirus subtype 3 replication in vitro. Journal of virology 2010, 84, 8903-8912.
61. Xu, C.; Guo, T.-C.; Mutoloki, S.; Haugland, Ø.; Evensen, Ø. Gene expression studies of host response to Salmonid alphavirus subtype 3 experimental infections in Atlantic salmon. Veterinary research 2012, 43, 1-10.
62. Gascoigne, N.R.; Zal, T.; Yachi, P.P.; Hoerter, J.A. Co-receptors and recognition of self at the immunological synapse. Immunological Synapse 2010, 171-189.
63. Wilson, A.B. MHC and adaptive immunity in teleost fishes. Immunogenetics 2017, 69, 521-528.
64. Li, J.; Barreda, D.R.; Zhang, Y.-A.; Boshra, H.; Gelman, A.E.; LaPatra, S.; Tort, L.; Sunyer, J.O. B lymphocytes from early vertebrates have potent phagocytic and microbicidal abilities. Nature immunology 2006, 7, 1116.
65. Bachmann, M.F.; Hengartner, H.; Zinkernagel, R.M. T helper cell-independent neutralizing B cell response against vesicular stomatitis virus: role of antigen patterns in B cell induction? European journal of immunology 1995, 25, 3445-3451.
66. Teige, L.H.; Aksnes, I.; Røsæg, M.V.; Jensen, I.; Jørgensen, J.; Sindre, H.; Collins, C.; Collet, B.; Rimstad, E.; Dahle, M.K. Detection of specific Atlantic salmon antibodies against salmonid alphavirus using a bead-based immunoassay. Fish & Shellfish Immunology 2020, 106, 374-383.
67. Salinas, I.; Fernández-Montero, Á.; Ding, Y.; Sunyer, J.O. Mucosal immunoglobulins of teleost fish: A decade of advances. Developmental & Comparative Immunology 2021, 121, 104079.

 doi:10.20944/preprints202310.1132.v1

disclaim responsibility for any injury to people or property resulting from any ideas, methods, instructions or products referred to in the content.